# Structural characterisation of two medium molecular mass exopolysaccharides produced by the bacterium *Lactobacillus fermentum* Lf2.

Hafiz I. Ahmed[a], Emma Ransom-Jones[b], Sohaib Sadiq[a], Ana Vitlic[b], Neil McLay[a,b], María F. Rojas[c], Elisa C. Ale[c], Ana G. Binetti[c], Andrew Collett[b], Paul N. Humphreys[b], Andrew P. Laws[a*]

[a]Department, of Chemical Sciences, University of Huddersfield, Queensgate, Huddersfield, HD1 3DH, United Kingdom;

[b]Department of Biological and Geographical Sciences, University of Huddersfield, Queensgate, Huddersfield, HD1 3DH, United Kingdom;

[c]Facultad de Ingeniería Química (UNL), Instituto de Lactología Industrial (UNL-CONICET), Santiago del Estero 2829, 3000 Santa Fe, Argentina.

*Corresponding Author.
Email address: a.p.laws@hud.ac.uk; Tel +44(0)1484472668; Fax +44(0)1484472182

## Abstract

Under optimized conditions, the lactic acid bacterium *Lactobacillus fermentum* Lf2 secretes up to 2 $gL^{-1}$ of a mixture of polysaccharides into the fermentation medium when grown on sucrose. Earlier studies had shown that the mixture is biologically active and work was undertaken to characterise the polysaccharides. Preparative size exclusion chromatography was used to separate a high molecular mass β-glucan (weight average mass of $1.23 \times 10^6$ $gmol^{-1}$) from two medium molecular mass polysaccharides (weight average mass of $8.8 \times 10^4$ $gmol^{-1}$). Under optimized growth conditions, the medium molecular mass polysaccharides accounted for more than 75% of the mixture by weight. Monomer, linkage analysis and NMR spectroscopy of the medium molecular mass polysaccharides, and material isolated after their Smith degradation, was used to identify the structure of the component polysaccharides. The mixture contains two novel polysaccharides. The first has a main chain of β-1,6-linked galactofuranoses which is non-stoichiometrically 2-*O*-glucosylated. The degree of substitution at the 2-position, with α-D-Glc*p,* depends on the fermentation conditions; under optimized conditions greater than 80% 2-*O*-α-D-glucosylation was observed.

$$\begin{array}{c} \rightarrow 6)\text{-}\beta\text{-D-Gal}f\text{-}(1\rightarrow \\ 2 \\ \uparrow \\ 1 \\ (\alpha\text{-D-Glc}p)_{0.8} \end{array}$$

The second polysaccharide is a heteroglycan with four monosaccharides in the repeat unit:

$$\begin{array}{l} \rightarrow 3)\text{-}\beta\text{-D-Glc}p\text{-}(1\rightarrow 3)\text{-}\beta\text{-D-Gal}f\text{-}(1\rightarrow 6)\text{-}\beta\text{-D-Gal}f\text{-}(1\rightarrow \\ \qquad\qquad\qquad\qquad\qquad\qquad\qquad\qquad\qquad\qquad\qquad\qquad\qquad\quad 2 \\ \qquad\qquad\qquad\qquad\qquad\qquad\qquad\qquad\qquad\qquad\qquad\qquad\qquad\quad \uparrow \\ \qquad\qquad\qquad\qquad\qquad\qquad\qquad\qquad\qquad\qquad\qquad\qquad\qquad\quad 1 \\ \qquad\qquad\qquad\qquad\qquad\qquad\qquad\qquad\qquad\qquad\qquad\qquad\qquad\quad \alpha\text{-D-Glc}p \end{array}$$

Residual signals in the NMR suggest that the sample also contains trace amounts (<3 %) of cell wall polysaccharides.


Keywords: Exopolysaccharide; LAB; Probiotic; Lactobacillus fermentum; NMR

## 1. Introduction

There is a long tradition of using Lactic Acid Bacteria (LAB) to generate fermented food products [1-3]. The fermentation process improves the desirability of the processed products either by increasing their resistance to spoilage [4-7] or by improving their physical attributes e.g. an increase in viscosity with associated changes in texture and mouth feel [8]. In the last decade, there has been renewed interest in the field of LAB and this has been driven by the recognition that many LAB cultures are probiotic organisms [9] i.e. they provide health benefits to the host when consumed. The identification of specific LAB strains as probiotic cultures has led to their being added to consumer products [10] [11]. Many of the health benefits associated with the consumption of probiotics have their origins in an improvement in gastrointestinal function [12].

A number of LAB strains secrete polysaccharides into their surrounding media during growth and these are referred to as exopolysaccharides (EPS) [13, 14]. It has previously been demonstrated that EPS can contribute to both the improved physical attributes of fermented foods [15] and to the health benefits assigned to the consumption of probiotic LAB strains [16, 17]. However, there are still significant gaps in knowledge of the molecular mechanisms by which EPS contribute to the health benefits. One of the difficulties in undertaking such studies is that probiotic LAB cultures frequently produce small amounts of EPS and they are often present as mixtures [18].

*Lactobacillus fermentum* Lf2 (*L. fermentum* Lf2) is a Gram-positive LAB culture that was isolated from semi-hard Tybo cheese [19]. It has previously been reported that *L. fermentum* Lf2 produces up to 2 $gL^{-1}$ of a mixture of polysaccharides when grown on sucrose under optimised conditions in a semi-defined medium [20]. It was also shown that the EPS mixture could improve the physical properties of fermented foods and protect mice against *Salmonella* infection [21].

93 Given that the EPS has desirable properties, we were interested in studying the chemical
94 composition of the EPS and in characterising the polysaccharides present. In an earlier study,
95 we reported that the crude EPS contains a mixture of both high and medium molecular mass
96 polysaccharides and identified the high molecular mass polysaccharide (HMMP) as a β-
97 glucan, which presented biological activity [22]. In this paper, we report the characterisation of
98 the medium molecular mass polysaccharides (MMMP).
99
100

## 2. Results and discussion

### *2.1. Composition of the EPS mixture produced by L. fermentum* Lf2

*L. fermentum* Lf2 secretes three different polysaccharides into the fermentation media when the culture is grown on sucrose. SEC-MALLS analysis of the crude product identified both a high molecular mass peak (HMMP; 1.23 x $10^6$ $gmol^{-1}$) and a broad medium molecular mass peak (MMMP; 8.8 x $10^4$ $gmol^{-1}$). The relative amounts of the polysaccharides present in the two fractions varied greatly as a function of the fermentation conditions: approximately equal amounts of HMMP & MMMP were isolated under non-optimized conditions whilst the MMMP fraction was favoured when the pH, nitrogen source and carbon feed were optimized (HMMP: MMMP; 1:3.84). Under optimized conditions, the yield of MMMP EPS approaches 1.6 $gL^{-1}$. It was possible to separate MMMP from HMMP by preparative size exclusion chromatography. MMMP eluted after two column volumes of mobile phase had been passed through the column and after HMMP had eluted.

### *2.2. Composition of MMMP.*

Monomer analysis of the MMMP fraction, either by analysis of monosaccharides by HPAEC-PAD or as their alditol acetates by GC-MS, confirmed that glucose and galactose were the main monosaccharides present, with the average ratio of glucose to galactose being 1.0:1.1. Small amounts of mannose, galactosamine and glucosamine were also detected but their combined peak area was typically less than 3% of the total and these are likely to be derived from small amounts of cell wall material generated during cell lysis. Absolute configuration analysis using Gerwig's method [23] confirmed that both glucose and galactose were of D-absolute configuration.

In the linkage analysis for the MMMP fraction, the GC-MS trace for the methylated alditol acetates contained two large peaks and three small peaks. The large peaks corresponded to

126 a 1,5-di-*O*-acetyl-2,3,4,6-tetra-*O*-methylhexitol (from a terminal hexopyranose) and to 1,2,4,6-
127 tetra-*O*-acetyl-3,5-di-*O*-methylhexitol (from a 1,2,6-linked hexofuranose). The three small
128 peaks were identified as being a 1,3,5-tri-*O*-acetyl-2,4,6-tri-*O*-methylhexitol (from a 1,3-linked
129 hexapyranose) 1,4,6-tri-*O*-acetyl-2,3,5-tri-*O*-methylhexitol (from a 1,6-linked hexafuranose)
130 and 1,3,4-tri-*O*-acetyl-2,5,6-tri-*O*-methylhexitol (from a 1,3-linked hexafuranose) respectively.
131 In addition to the analysis of the native MMMP, monomer analysis was also carried out on a
132 sample of polysaccharide recovered after Smith degradation [24] of MMMP; here after
133 referred to as SD-MMMP. The GC trace for the mixture of alditol acetates generated from the
134 SD-MMMP contained three peaks: a small early eluting peak having a MS corresponding to a
135 five carbon alditol acetate derived from a pentose (generated during the oxidation-reduction of
136 the C5-C6 vicinal diol present in the 1,3-linked hexafuranose); a small 1,2,3,4,5,6-hexa-*O*-
137 acetylglucitol peak and a large 1,2,3,4,5,6-hexa-*O*-acetylgalactitol peak were also present.
138 *2.3 NMR analysis of the SD-MMMP.*
139 To simplify the structural characterisation, it was decided to start by determining the structures
140 of the products generated via Smith degradation of the native MMMP. In the Smith
141 degradation process reported here, the MMMP were subjected to oxidation, reduction, mild
142 acid hydrolysis and the final sample was dialysed. If the main back-bone of the repeat unit is
143 resistant to oxidation then a high molecular mass material would be recovered from inside the
144 dialysis tubing. In contrast, if any of the residues in the main chain are oxidized then
145 oligosaccharides could potentially be generated and these would pass through the dialysis
146 tubing. In the current experiments, a significant proportion of the products was retained within
147 the dialysis tubing suggesting that the main chain/s present in SD-MMMP are mostly resistant
148 to oxidation. The latter result is consistent with the presence of 1,2,6-linked furanoses, 1,3-
149 linked furanoses and 1,3-linked pyranoses in the linkage analysis which must be present in
150 the main chain/s of MMMP. The different batches of SD-MMMP provided $^{1}$H-NMR spectra

(Fig 1; F2-axis) with very similar patterns of anomeric signals: three small signals at 5.23, 5.00 and 4.53 ppm (labelled **A**, **B** and **D** in order of reducing chemical shifts) and one large signal at 4.96 ppm (labelled as **C**). The integrals for the small signals were, within experimental error, the same. However, the integral for the large signal **C** (compared to that of the small signals) varied from batch to batch: the integral ratio **C**/**A** varied from 3.31 to 4.52. The simplest explanation for the latter observation, and the results of subsequent studies on the parent MMMP (see discussion below) is that two different polysaccharides are present in MMMP.

Figure 1

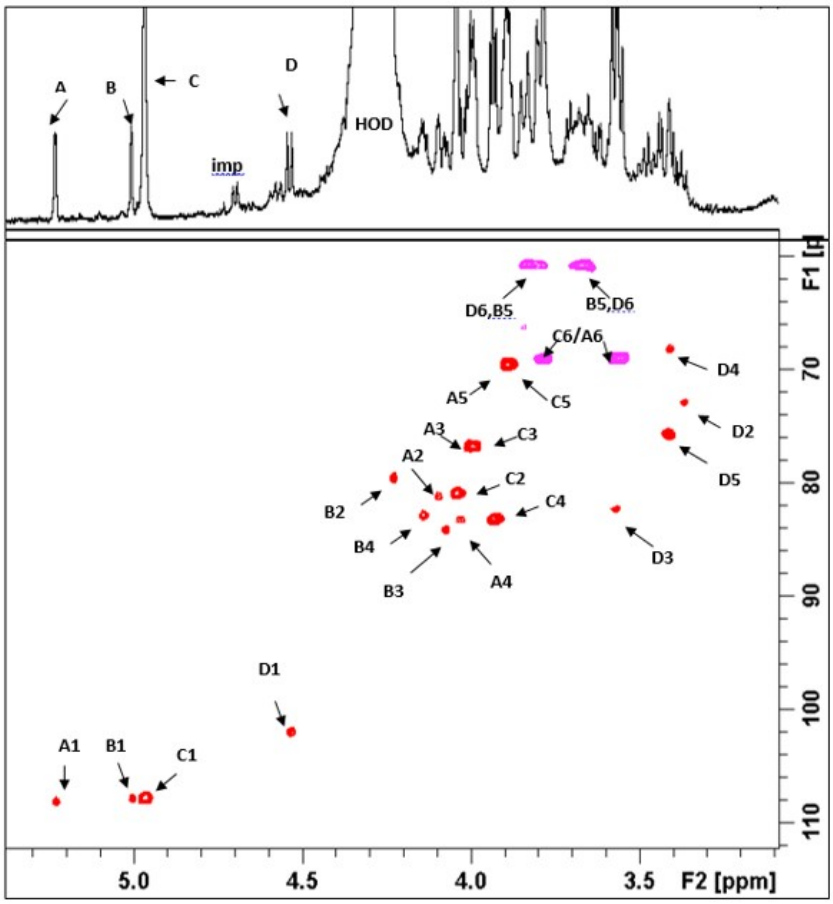


**Fig 1.** Top (F2-axis) $^{1}H$ NMR spectrum for the *L. fermentum* Lf2- SD-MMMP recorded at 70 $^{o}C$ on a Bruker 600 MHz spectrometer; Bottom-a $^{1}H$ ,$^{13}C$ ed-HSQC spectrum (Black contours = CH; Magenta contours =$CH_2$) for SD-MMMP; labels (**A-D**) identify the

different monosaccharides and the numbers (**1-6**) identify the respective protons/carbons. Imp=impurity observed in this batch but not in subsequent batches. In order to characterise the polysaccharides, the chemical shifts for the H1-H6 protons in the monosaccharides **A-D** were determined by tracking scalar coupling, using a combination of a COSY and TOCSY spectrum (not shown). The corresponding carbon chemical shifts were determined using an edited HSQC spectrum (Fig. 1) and a combination of the edited HSQC spectrum (Fig 2; red contours CH, magenta contours $CH_2$) with a HSQC-TOCSY spectrum (Fig 2. black contours).

Figure 2

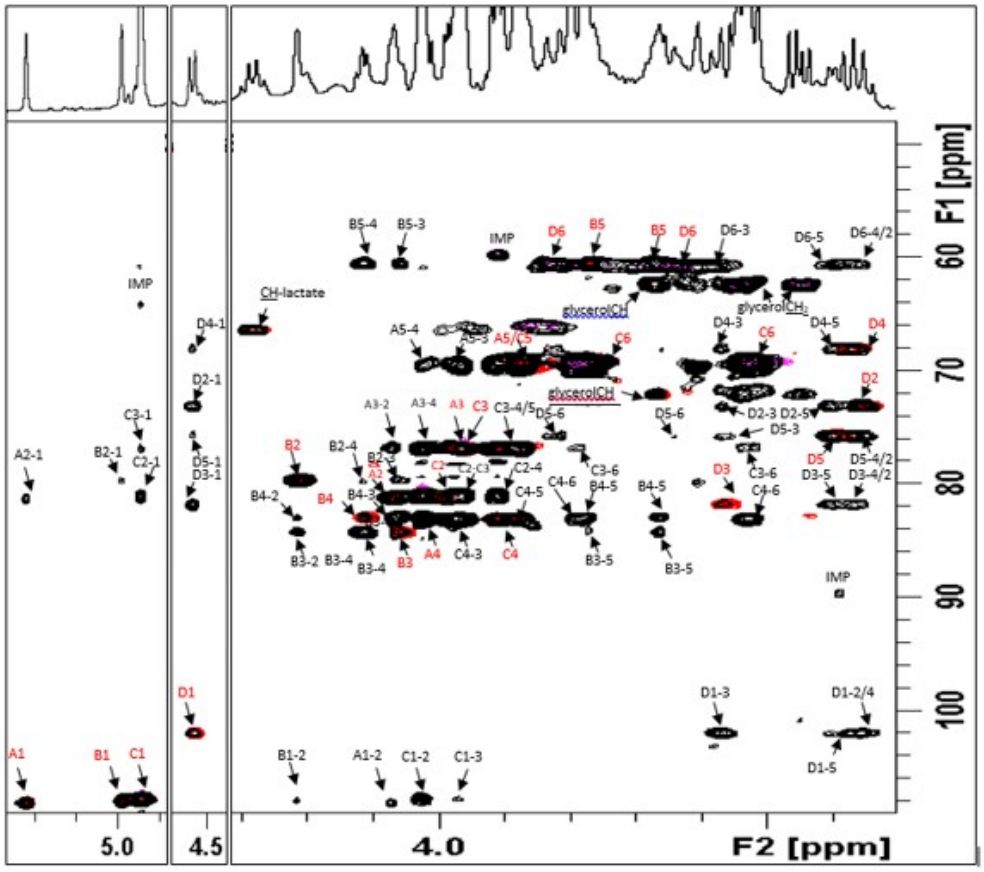


**Fig. 2.** Selected regions of $^{13}C,^{1}H$-HSQC-TOCSY (black contours) superimposed on top of an $^{13}C,^{1}H$-ed-HSQC (Red contours = CH; Magenta contours =$CH_2$) spectrum for *L. fermentum* Lf2 SD-MMMP recorded at 30 °C on a Bruker 600 MHz spectrometer; labels

(**A-G**) identify the different monosaccharides and the numbers (**1-6**) identify the respective protons/carbons. Red labels (A-G; 1-6) identify overlap of HSQC and HSQC-TOCSY signals. Imp=impurity; mainly spectral noise and often not correlated to either a carbon or hydrogen. Glycerol is an impurity entering the system during dialysis

The chemical shifts of the individual protons and carbons, in each of the different monosaccharides, are included in table 1 and highlighted on the HSQC spectrum (Fig. 1).

**Table 1.**

| Residue | | C-1 | C-2 | C-3 | C-4 | C-5 | C5b | C-6 |
|---|---|---|---|---|---|---|---|---|
| | | *H-1* | *H-2* | *H-3* | *H-4* | *H-5* | *H-5b* | *H-6s* |
| →6)-β-D-Gal*f*-(1→ | **A** | 108.1<br>*5.23* | 81.2<br>*4.10* | 76.7<br>*4.01* | 83.1<br>*4.03* | 69.5*<br>*3.90* | | 69.1<br>*3.81 & 3.60* |
| →3)-β-L-Ara*f*-(1→ | **B** | 107.8<br>*5.00* | 79.6<br>*4.23* | 84.0<br>*4.07* | 82.8<br>*4.14* | 60.6<br>*3.77* | 3.67 | NA |
| →6)-β–D-Gal*f*-(1→ | **C** | 107.8<br>*4.96* | 80.9<br>*4.04* | 76.8<br>*3.98* | 83.2<br>*3.93* | 69.7*<br>*3.85* | | 69.3<br>*3.81, 3.59* |
| →3)-β-D-Glc*p*-(1→ | **D** | 101.9<br>*4.53* | 72.8<br>*3.37* | 82.2<br>*3.57* | 68.0<br>*3.41* | 75.8<br>*3.42* | | 60.7<br>*3.82 & 3.65,* |

$^{1}$H and $^{13}$C NMR chemical shifts (δ, ppm) of the *L. fermentum* Lf2- SD-MMMP recorded in D2O at 70 °C and using acetone as internal/external reference. Signals labelled with * could not be assigned definitively and should be considered as interchangeable.

The assignment of the NMR resonances to the individual monosaccharides started from inspection of the location of the H-4 protons. In galactose the chemical shifts of H-4 protons occur above 3.9 ppm [25], whereas those in glucose occur below 3.5 ppm which indicates that residue **D** is the only glucose present. The downfield chemical shift of C-3 of **D** and the $^{3}J_{H1\text{-}H2}$ coupling constant of 8.0 Hz is consistent with **D** being a 1,3-β-linked D-glucopyranoside. Residue **B** is a five carbon sugar (L-arabinose) generated during Smith degradation of a 1,3-linked D-galactofuranose in the parent polysaccharide. The chemical shifts for **B** C-1 and C-3 are very similar to those reported for a β-1,3-linked-L-arabinose in an arabinan oligosaccharide reported by Wefers *et al* [26] : C-1 107.9 ppm and C-3 84.5 ppm.

The location of the C-1 to C-4 resonances in residues **A & C** are typical of those of β-galactofuranosides and the downfield shifts of both their C-6s identifies these as 1,6-β-D-Gal*f*s [27].

In order to check if any oligosaccharides were produced during the Smith degradation, the final dialysate was freeze-dried and NMR spectra recorded (not shown). In addition to large lactate and glycerol resonances, signals matching those of **C** i.e. a 1,6-β-D-Gal*f* were present, this suggests that a small amount of a low molecular mass polysaccharide or an oligosaccharide was escaping from the dialysis tubing. One possible explanation for the latter result is that the small number of 1,6-linked galactofuranoses, identified in the linkage analysis, are present in the back-bone of one of the two polysaccharides in MMMP. Following Smith degradation, the chain will cleave at this point leading to a reduction in molecular weight of the MMMP containing residue **C**. The observation of different patterns of anomeric NMR signals inside (**A, B, C** and **D**) and outside (**C** only) of the dialysis tubing is consistent with two polysaccharides being present in SD-MMMP. The first polysaccharide, SD-MMMP1, is composed of a linear chain of 1,6-β-D-Gal*f*s:

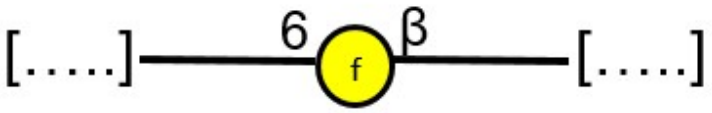


**C**

The second polysaccharide, SD-MMMP2, contains the residues **A**, **B** and **D**. To identify the structure of the polysaccharide SD-MMMP2, the order of the residues in the repeat unit was determined by inspection of inter and intra-residue correlations, observed between residues **A**, **B** and **D,** in both ROESY and HMBC spectra and these are listed in Table 2.

**Table 2.**

| Anomeric proton in sugar residue (δ) | NOE Correlations to protons in sugar residues (δ) |
|---|---|
| **A** H-1 (5.23) | **A H-2 (4.10)**, **A** H-3 (4.01), **D H-3 (3.57).** |
| **B** H-1 (5.00) | **B H-2 (4.23)**, **B** H-3 (4.07) **A H-6a (3.81), A H-6b (3.60).** |
| **D** H-1 (4.53) | B H-2 (4.23), **B H-3 (4.07), D** H-3(3.57), **D** H-5 (3.42), **D** H-2 (3.37), |
| | **HMBC Correlations to carbons in sugar residues (δ)** |
| **A** H-1 (5.23) | **A** C-4 (83.1), **D C-3 (82.2).** |
| **B** H-1 (5.00) | **B** C-4 (82.8), **A C-6 (69.1).** |
| **D** H-1 (4.53) | **B** C-3 (84.0), |

Strong (Bold) and medium strength (Grey) correlations for H-1 in the 600-MHz 2D $^{1}$H,$^{1}$H ROESY spectrum (TOP) and $^{1}$H-$^{13}$C-HMBC spectrum (Bottom) for *L. fermentum* Lf2- SD-MMMP.

On the ROESY and HMBC spectra, inter-residue correlations are observed between **A** H-1 and **D** H-3 and between **A** H-1 and **D** C-3 respectively, identifying a 1,3-linkage between the two. A similar pattern of inter-residue correlations is observed from **D** H-1 to **B** H-3 on the ROESY spectrum and **D** H-1 to **B** C-3 on the HMBC spectrum, indicating that **D** and **B** are also joined by a 1,3-linkage. The observation of a correlation between **B** H1 and protons at 3.81 pmm and 3.60 ppm is consistent with **B** forming a 1,6-link to **A**.

Given the correlations observed in the HMBC and the ROESY spectra, the structure for the SD-MMMP2 is:

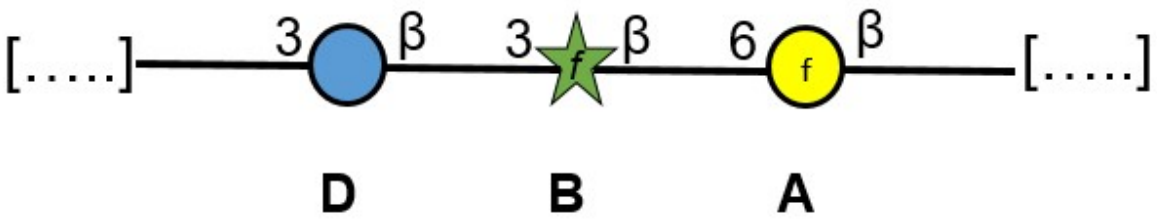

*2.4 NMR analysis of the native-MMMP.*

The anomeric region of the $^{1}$H-NMR spectrum of the native MMMP has seven signals. Four of which (**A-D**) are derived from the backbone residues observed in SD-MMMP1 (**C**) & SD-MMMP2 (**A,B and D**) see discussion below. The three remaining signals are labelled **F, G** and **E** (Fig 3, F2-axis). Within error, **F** has the same integral as **A**, and **G** has a similar but slightly smaller integral than that of **C**. In the different batches of MMMP, the integral area for **E** was very variable and was sometimes lower than that of **A** whilst in other batches, recovered from different fermentations, the integral area for **E** was significantly larger than that of **A**. The variable integrals again suggest that more than one polysaccharide is present. Unfortunately, all attempts to separate the mixture, using smaller pore-size size exclusion columns and using an anion exchange column, failed. Therefore, it was decided to directly characterise the different polysaccharides *in-situ* i.e. as components of a mixture.

As was the case for the SD-MMMP, the location of the protons H-1 to H-6 was determined from inspection of a combination of the COSY and TOCSY spectra (not shown). The location of the carbons C-1 to C-6 was determined from inspection of an ed-HSQC spectrum (Fig. 3) and of a combination of a HSQC spectrum (Fig. 4; red contours) and a HSQC-TOCSY spectrum (Fig. 4; black contours). The location of the individual resonances are listed in table 3 and highlighted on the ed-HSQC spectrum (Fig 3). The chemical shifts for the protons H-2 to H-6 and carbons C-2 to C-6 in **F** and **G** are very similar and it was not possible to differentiate between the two sets of resonances**.**

Figure 3:

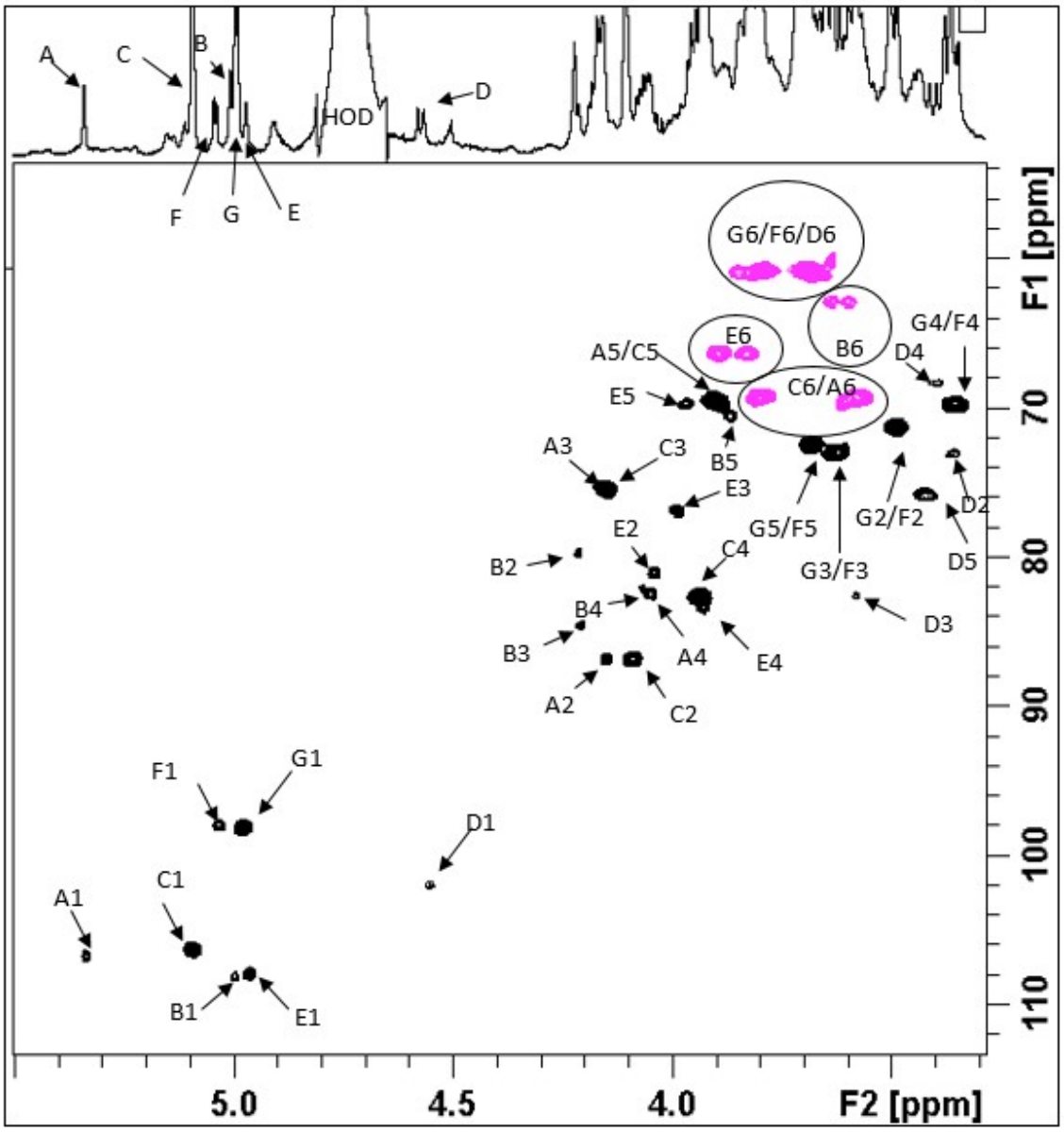


Top (F2-axis) $^{1}H$ NMR spectrum for the *L. fermentum* Lf2- MMMP recorded at 30 $^{o}C$ on a Bruker 600 MHz spectrometer; Bottom-a $^{1}H$ ,$^{13}C$ ed-HSQC spectrum (Black contours = CH; Magenta contours =$CH_2$) labels (**A-G**) identify the different monosaccharides and the numbers (**1-6**) identify the respective protons/carbons

The chemical shift of **F** and **G** H-4 at < 3.4 ppm and the $^{3}J_{H1\text{-}H2}$ coupling constants of 3.4 Hz and 3.6 Hz respectively are consistent with these two residues being alpha-linked glucoses

[25]. The location of the carbons C-2 to C-5 are very close to those reported in the literature for methyl-*O*-D-glucopyranoside [27] which suggests that **F** and **G** are the terminal glucopyranoses observed in the MMMP linkage analysis.

Figure 4

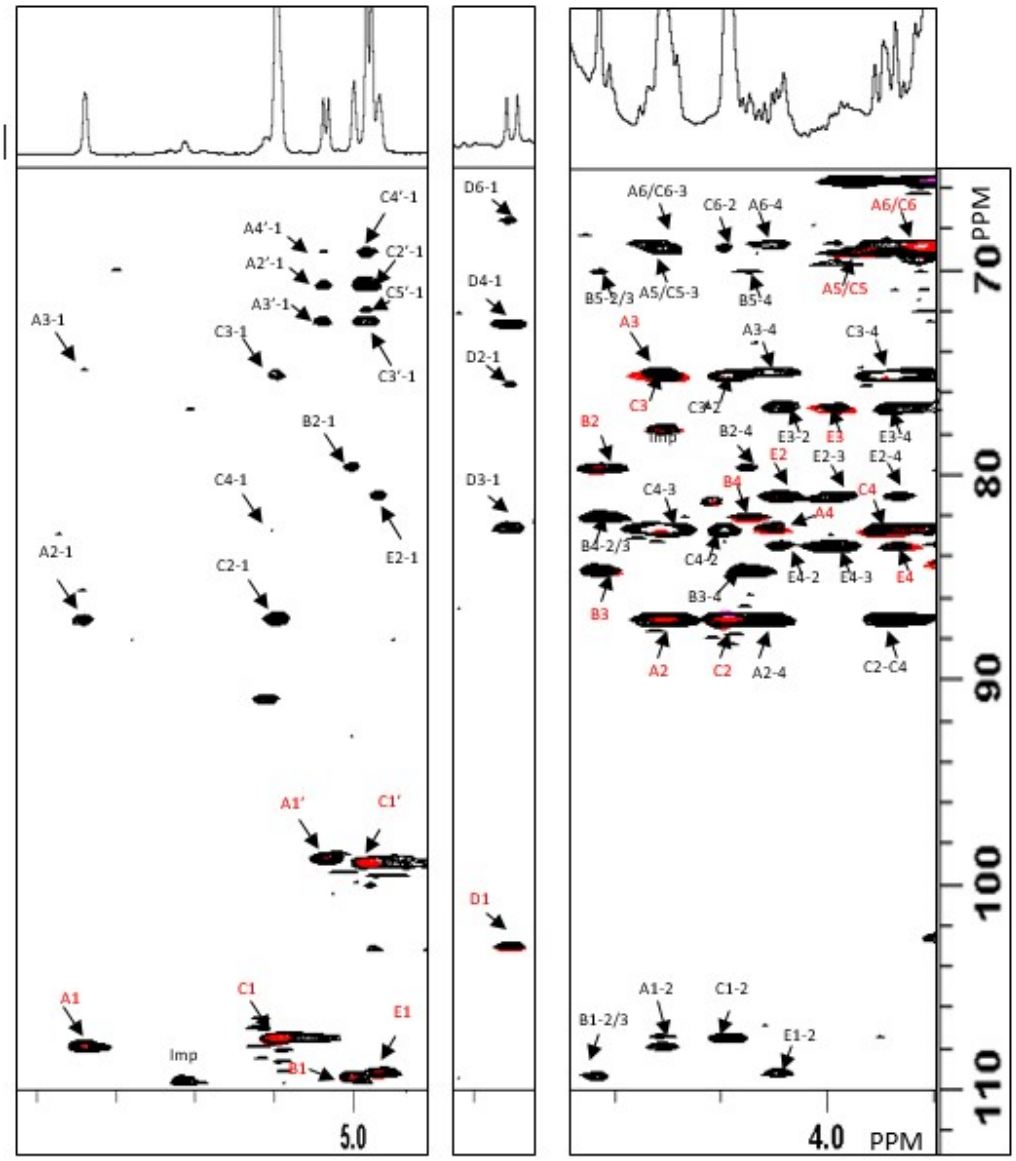


**Fig. 4.** Selected regions of $^{13}C,^{1}H$-HSQC-TOCSY (black contours) superimposed on top of an $^{13}C,^{1}H$-ed-HSQC (Red contours = CH; Magenta contours =$CH_2$) spectrum for *L. fermentum* Lf2 MMMP recorded at 70 °C on a Bruker 600 MHz spectrometer; labels (**A-**

**E & A',C'**) identify the different monosaccharides and the numbers (**1-6**) identify the respective protons/carbons. Red labels (A-G; 1-6) identify overlap of HSQC and HSQC-TOCSY signals. Imp=impurity-possibly cell wall material.

**Table 3.**

| Residue | | C-1 | C-2 | C-3 | C-4 | C-5 | C-6 |
|---|---|---|---|---|---|---|---|
| | | *H-1* | *H-2* | *H-3* | *H-4* | *H-5* | *H-6s* |
| →2,6)-β-D-Gal*f*-(1→ | **A** | 107.0<br>*5.34* | 87.2<br>*4.15* | 75.8<br>*4.15* | 83.0<br>*4.05* | 69.9*<br>*3.91* | 69.7<br>*3.80 & 3.58* |
| α-D-Glc*p*-(1→ | **F** | 98.3<br>5.03 | 71.7#<br>3.50 | 73.3#<br>3.63 | 70.3#<br>3.36 | 72.9#<br>3.69 | 61.2#<br>3.80 & 3.69 |
| →,3)-β-D-Gal*f*-(1→ | **B** | 108.5<br>*5.00* | 80.1<br>*4.22* | 84.9<br>*4.21* | 82.5<br>*4.07* | 70.8<br>*3.87* | 63.3<br>*3.64 & 3.60* |
| →2,6)-β–D-Gal*f*-(1→ | **C** | 106.7<br>*5.09* | 87.3<br>*4.09* | 75.8<br>*4.12* | 83.1<br>*3.94* | 69.8<br>*3.91* | 69.7<br>*3.81 & 3.58* |
| α-D-Glc*p*-(1→ | **G** | 98.6<br>4.98 | 71.7#<br>3.50 | 73.3#<br>3.63 | 70.3#<br>3.36 | 72.9#<br>3.69 | 61.2#<br>3.80 & 3.69 |
| →3)-β-D-Glc*p*-(1→ | **D** | 102.5<br>*4.55* | 73.6<br>*3.36* | 83.0<br>*3.59* | 68.7<br>*3.41* | 76.2<br>*3.42* | 61.3<br>*3.80 & 3.68* |
| →6)-β-D-Gal*f*-(1→ | **E** | 108.4<br>*4.97* | 81.4<br>*4.05* | 77.4<br>*3.99* | 83.8<br>*3.93* | 70.0<br>*3.98* | 66.8<br>3.90 & 3.84 |

$^{1}$H and $^{13}$C NMR chemical shifts (δ, ppm) of the *L. fermentum* Lf2-MMMP recorded in D2O at 70 °C and using acetone as internal/external reference. Signals labelled with# (in the same column) occur at the same location.

The point of attachment of the two t-α-D-Glc*p*s to the main chain of the MMMPs was determined from inspection of the inter- and intra-residue correlations observed on ROESY and HMBC spectra which are listed in Table 4. Strong NOEs were observed between **F-1** and **A-2**, and between **G-1** and **C-2**. The inter-residue correlation data suggests that the t-D-Glc*p* **F** is bonded to the 2-position of **A** and, likewise, **G** is bonded to the 2-position of **C.**

| Anomeric proton in sugar residue (*δ*) | NOE Correlations to protons in sugar residues (*δ*) |
|---|---|
| **A** H-1 (5.34) | **F H-1 (5.03) A H-2 (4.15) D H-3 (3.59).** |
| **C** H-1 (5.09) | **G H-1 (4.98)**, **C** H-3 (4.12) **C** H-2 (4.09) **C** H-5 (3.91) **A/C H-6a (3.81), A/C H-6b (3.58).** |
| **F** H-1 (5.03) | **A H-1 (5.34) A H-2 (4.15) F/G** H-2 (3.50). |
| **B** H-1 (5.00) | **B** H-3 (4.21), **A/C H-6a (3.80-3.81), A/C H-6b (3.60-3.58).** |
| **F** H-1 (4.98) | **C H-1 (5.09) C H-2 (4.09) G/F** H-2 (3.50). |
| **E** H-1 (4.97) | **A/C H-6a (3.80-3.81), A/C H-6b (3.60-3.58).** |
| **D** H-1 (4.55) | **B H-3 (4.21), D** H-3(3.59), **D** H-5 (3.42). |
| | **HMBC Correlations to carbons in sugar residues (*δ*)** |
| **A** H-1 (5.34) | **A** C-4 (83.0) or **D C-3 (83.0).** |
| **C** H-1 (5.09) | **C** C-2 (87.3), **C/A** C-3 (75.8), **C** C-4 (83.1), **C/A C-6 (69.7).** |
| **F** H-1 (5.03) | **A C-2 (87.2) F/G** C-2 (71.7) |
| **B** H-1 (5.00) | **B** C-4 (82.5), **A C-6 (69.7).** |
| **G** H-1 (4.98) | **C C-2 (87.3) G/F** C-3 (73.3). |
| **E** H-1 (4.97) | **E** C-4 (83.8) **A/C C-6a (69.7)** |
| **D** H-1 (4.55) | **B C-3 (84.9)** |

**Table 4.** Strong (Bold) and medium strength (Grey) correlations for H-1 in the 600-MHz 2D $^{1}$H,$^{1}$H ROESY spectrum (TOP) and $^{1}$H-$^{13}$C-HMBC spectrum for *L. fermentum* Lf2- MMMP.

The only signals unaccounted for are those belonging to **E,** these were absent in SD-MMMP. The chemical shifts of the **E** H-4 proton at $\delta$ > 3.9 ppm and carbon C-6 at 67 ppm are consistent with **E** being the 1,6-linked $\alpha$-D-Gal*f* observed in the linkage analysis. The location of **E** in MMMP was identified from the inter residue correlations observed in the ROESY and HMBC spectra (Table 4). Correlations were observed between **E** H-1 to either **A** or **C** H-6/C-6 (ROESY/HMBC). Given that the integral area for **E** often exceeded that of **A** it is more likely that **E** is linked to **C** C-6. The presence of a vicinal diol (2-OH, 3-OH) in **E** means that **E** would be expected to react with the periodate used in the Smith degradation. After reduction and mild acid hydrolysis, the C3-C6 carbons of **E** would be expected to give a molecule of D-threitol linked to the anomeric carbon of the neighbouring monosaccharide, **C,** and this would

be part of a low molecular weight polysaccharide or oligosaccharide and, as such, this would account for the material which was recovered from the Smith degradation diasylate.

Again, the combined results of the NMR, monomer and linkage analysis, can be explained by considering MMMP as being composed of two polysaccharides. The first, MMMP1, has a main chain of 1,6-linked β-Gal*f*s, the majority of which have a terminal α-D-Glc*p* attached at the 2-position. However, the 2-*O*-glucosylation is not stoichiometric and a small number of unsubstituted 1,6-linked β-Gal*f*s are present. MMMP1 has the following structure:

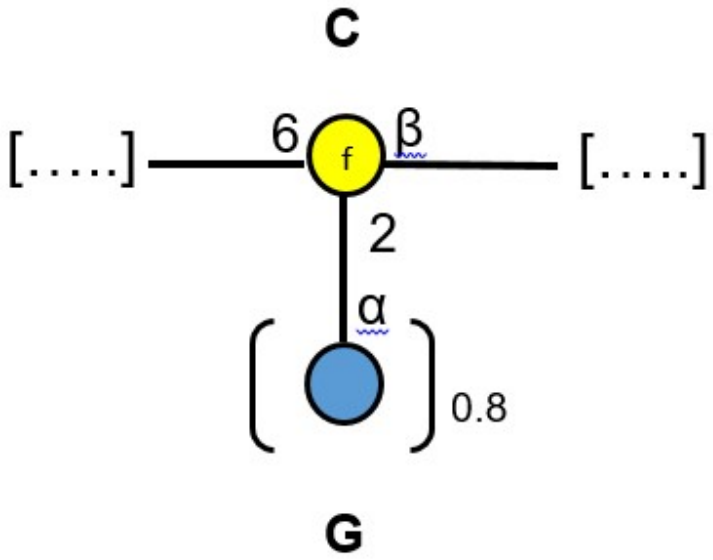


The extent to which the 2-*O*-glucosylation is absent is dependent on the fermentation conditions.

The second polysaccharide, MMMP2, is similar to SD-MMMP2 (with Gal replacing Ara) but has a terminal α-D-Glc*p* attached at the 2-position of **A**:

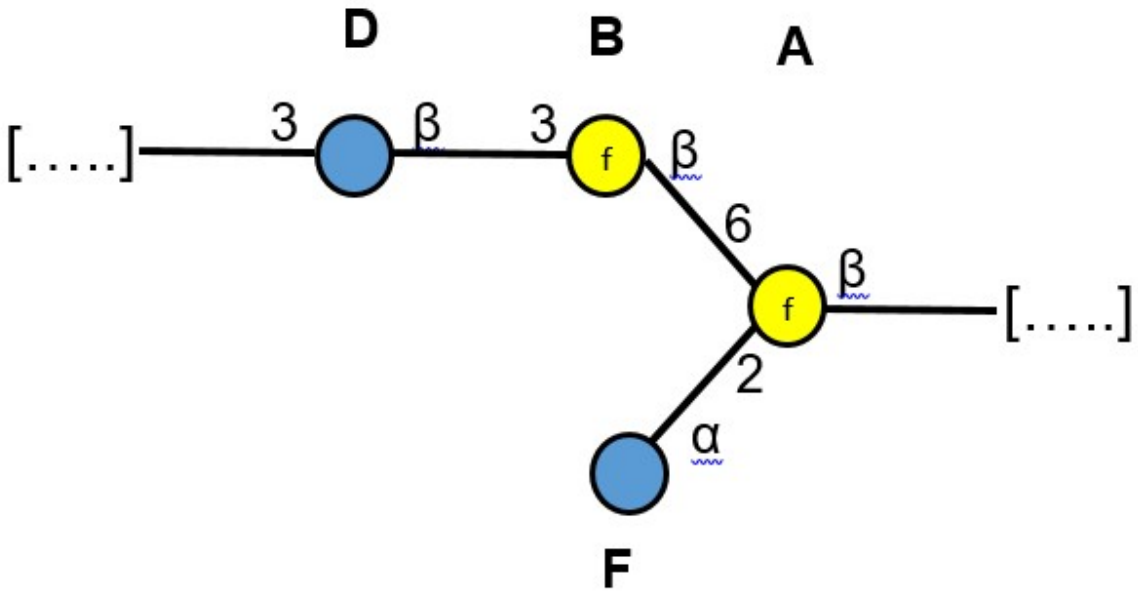


342

343

344 A search of the scientific literature and the Bacterial Carbohydrate Structure Database [28]
345 suggests that the two medium molecular mass EPS have novel structures. However, it is
346 worth noting that the LPS isolated from *Acetobacter pasteurianus* CIP103108 [29] has a
347 repeat unit which contains part of the repeat unit of MMP2 i.e. residues **B, A, F**. However, in
348 the *Acetobacter pasteurianus* CIP103108 there is non-stoichiometric glycosylation at the 2-
349 position of **A**.

350

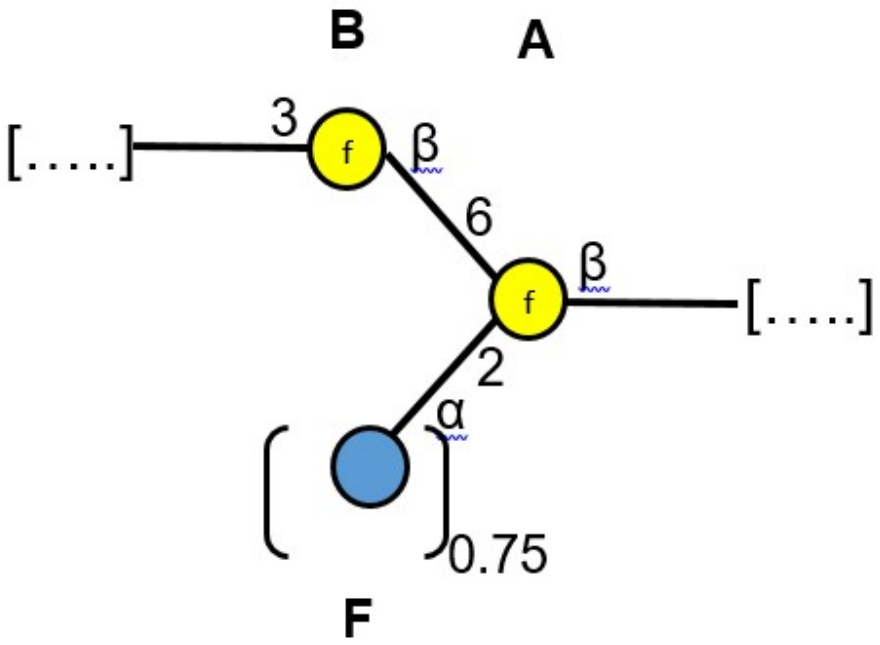


Both MMMP polysaccharides have backbones containing β-D-Gal*f* . β-D-Gal*f* is a relatively ubiquitous structural element in bacterial polysaccharides, a search of the Bacterial Carbohydrate Structural Database [28] identified 206 polysaccharides containing 1,6-linked D-Gal*f*.

We have performed a number of assays to determine the biological activity of the medium molecular mass polysaccharides; these provisional studies have shown that the polysaccharides are able to influence the release of the inflammatory cytokine TNF-α from peripheral mononuclear blood cells. However, because of the presence of a small amount of cell wall material within the MMMP fraction, it is not possible to say which of the polysaccharides is responsible for the biological activity. Further work is under way in an attempt to remove the cell wall polysaccharides and the results will be published elsewhere.

In conclusion, under optimum growth conditions *L fermentum Lf2* secretes both a high molecular mass β-glucan and a mixture of two novel medium mass heteropolysaccharides (MMMP1 & MMMP2) into the fermentation medium. As significant amounts of each of these

368 polysaccharides are produced, it should be possible to determine their physical and biological
369 activity. We have previously demonstrated that the *L fermentum* Lf2 β-glucan is able to
370 modulate the release of the pro-inflammatory cyctokine TNF-α. Our provisional studies of the
371 biological activity of the medium molecular mass polysaccharides suggest that there is a
372 functional interaction between the novel EPS and peripheral mononuclear blood cells. We are
373 currently investigating a range of methods for separating MMMP1 and MMP2 (and for
374 removing the residual cell wall material) in order to be able to investigate the properties of the
375 individual polysaccharides.

376 3. **Experimental**

377 *3.1 Materials.*

378 Unless otherwise stated, reagents were purchased from the Sigma-Aldrich Company Ltd.
379 (Poole, Dorset UK) and were used as supplied.

380 *3.2 EPS production and purification of the crude EPS mixture.*

381 *L. fermentum* Lf2 was grown at the Instituto de Lactología Industrial (Santa Fe, Argentina).
382 The procedures used to produce and isolate the crude EPS have already been reported [19,
383 21]. The different polysaccharides in the crude EPS mixture were separated by size exclusion
384 chromatography on a Sephacryl S-500 HR column (XK26/60-GE Healthcare, Fisher Scientific,
385 UK) eluting with ultrapure water (flow rate 5.0 mL $min^{-1}$). Sixty 5 mL fractions were collected
386 with the location of polysaccharides being determined by measuring the carbohydrate content
387 of each fraction [30, 31]. The sample eluted as two main peaks: HMMP eluted in the early
388 fractions and MMMP eluted in tubes 25-30. The characterisation of the structure of the HMMP
389 has already been reported [22].

390 *3.3 Determination of the purity of the MMMP EPS fraction and its weight average molecular*
391 *mass.*

392 Size Exclusion Chromatography coupled with Multi-Angle Laser Light Scattering (SEC-
393 MALLS-Wyatt technology, Santa Barbara, CA, USA) was used to determine the purity of the
394 fractions; the procedures employed have been reported in a previous paper [22]. Briefly, EPS
395 (1 mg.mL$^{-1}$) were prepared in aq. $NaNO_3$ (0.1M) and stirred for 16 h to ensure the EPS was
396 completely dissolved. Samples (100 µL) were injected, in triplicate, into a SEC-MALLS
397 system (three columns connected in series: PL Aquagel-OH 40, 50 and 60 (8 µm, 30 cm x 7.5
398 mm, Agilent, Cheadle, UK)) with a flow rate of 0.7 mL.min$^{-1}$. A differential refractometer
399 (Optilab rEX, Wyatt technology, Santa Barbara, CA, USA) was used to determine the
400 concentration of the polysaccharide and a Dawn-EOS MALLS detector (operating at 690 nm)
401 was used to determine the weight average molecular mass of the polysaccharide. An in-line
402 UV detector (Shimadzu, Milton Keynes, UK) was used for the detection of proteins and
403 nucleic acid impurities. ASTRA version 6.0.1 software (Wyatt technology, Santa Barbara, CA,
404 USA) was used for the data analysis.

405 *3.4 Composition of MMMP*.

406 The monosaccharides present in the MMMP fraction and in the EPS that had been
407 subjected to Smith oxidation (see section 3.5; SD-MMMP) were determined after acid
408 hydrolysis using both HPAEC-PAD analysis and GC-MS analysis of the corresponding alditol
409 acetates, as previously described [32]. The absolute configuration of the MMMP sugars was
410 determined by preparation of their respective 2-(*S*)-butylglycosides using Gerwig's method
411 [23]. For linkage analysis, both MMMP and SD-MMMP were permethylated using the
412 procedures described by Stellner et al [33].

413 *3.5 Smith degradation of MMMP.*

414 The Smith degradation of MMMP was performed using the procedures described by Abdel-
415 Akher et al [24]. The MMMP EPS (37 mg) was dissolved in sodium acetate buffer (0.1M, pH
416 3.9, 25 mL) and sodium periodate (0.2 M, 8.5 mL) was added. The sample tube was wrapped

417 in silver foil and stored in the dark at 4 $^{o}$C for 120 h. After 120 h, excess periodate was
418 destroyed by adding ethylene glycol (2 mL). The reaction mixture was transferred to a dialysis
419 bag and the contents dialysed against ultra-pure water (500 mL) for 24 h. After 24 h, the
420 contents of the dialysis bag were isolated and sodium borohydride (200 mg) was added and
421 left for 4h after which time excess borohydride was decomposed by careful addition of acetic
422 acid until the pH reached 4.5. The oxidized-reduced sample was dialysed again against
423 ultrapure water (500 mL) for 24 h and the contents of the dialysis bag were freeze-dried.
424 Finally, the oxidized and reduced EPS sample was stirred with aqueous TFA (0.5 M) for 24 h
425 at room temperature after which time the resulting solution was evaporated to dryness under
426 an atmosphere of nitrogen at 60 $^{o}$C and the sample was dialysed again against ultrapure
427 water (500 mL) for 24 h and both the contents of the dialysis bag and the dialysate were
428 freeze-dried.
429 *3.5 NMR spectroscopy*.
430 Samples of MMMP or SD-MMMP (5-10 mg) from a number of fermentations, were dissolved
431 directly in $D_2O$ (650 μl, Goss Scientific Instruments Ltd., Essex). NMR spectra were recorded
432 at a either room temperature or at 70 °C unless otherwise stated. The elevated temperature
433 shifted the residual HOD signal to higher field, into a clear region of the spectrum. The higher
434 temperature also improved spectral resolution by reducing the sample viscosity. The NMR
435 spectra were recorded on a Bruker Avance Neo 600 MHz $^{1}$H (150 MHz $^{13}$C) spectrometer
436 fitted with a cold probe (liquid nitrogen cooled) operating with Z-field gradients where
437 appropriate and using Bruker's pulse programmes. Chemical shifts are expressed in ppm
438 relative to either internal or external acetone; δ 2.225 for $^{1}$H and δ 31.55 for $^{13}$C. The 1D $^{1}$H
439 and $^{13}$C spectra were processed with 65,536 data points. The 2D gs-DQF-COSY spectra
440 were recorded in magnitude mode at 70 °C. The TOCSY experiments were recorded with
441 mixing times of either 80 or 120 ms. The 2D-heteronuclear $^{1}$H-$^{13}$C ed-HSQC, and phase

sensitive HSQC-TOCSY (80 ms) were recorded using Bruker pulse sequences and either 256, 512 or 1024 experiments of 2048 data points. The ROESY spectrum was recorded using Bruker '2D EASY ROESY' pulse sequence and 256 experiments of 1024 data points.

For the majority of spectra, time-domain data were multiplied by phase-shifted (squared-) sine-bell functions.

**References:**


[1] F. Leroy, L. De Vuyst, Lactic acid bacteria as functional starter cultures for the food fermentation industry, Trends Food Sci. Technol. 15(2) (2004) 67-78.

[2] A. Lonvaud-Funel, Lactic acid bacteria in the quality improvement and depreciation of wine, in: W.N. Konings, O.P. Kuipers, J.H.J.H. In 't Veld (Eds.), Lactic Acid Bacteria: Genetics, Metabolism and Applications: Proceedings of the Sixth Symposium on lactic acid bacteria: genetics, metabolism and applications, 19–23 September 1999, Veldhoven, The Netherlands, Springer Netherlands, Dordrecht, 1999, pp. 317-331.

[3] M.E. Stiles, Biopreservation by lactic acid bacteria, Antonie van Leeuwenhoek 70(2) (1996) 331-345.

[4] D.K.D. Dalié, A.M. Deschamps, F. Richard-Forget, Lactic acid bacteria – Potential for control of mould growth and mycotoxins: A review, Food Control 21(4) (2010) 370-380.

[5] L. De Vuyst, E.J. Vandamme, Antimicrobial Potential of Lactic Acid Bacteria, in: L. De Vuyst, E.J. Vandamme (Eds.), Bacteriocins of Lactic Acid Bacteria: Microbiology, Genetics and Applications, Springer US, Boston, MA, 1994, pp. 91-142.

[6] S. Rouse, D. Van Sinderen, Bioprotective potential of lactic acid bacteria in malting and brewing, J. Food Prot. 71(8) (2008) 1724-1733.

[7] S.J. Sathe, N.N. Nawani, P.K. Dhakephalkar, B.P. Kapadnis, Antifungal lactic acid bacteria with potential to prolong shelf-life of fresh vegetables, J. Appl. Microbiol.103(6) (2007) 2622-2628.

[8] V.M. Marshall, H.L. Rawson, Effects of exopolysaccharide-producing strains of thermophilic lactic acid bacteria on the texture of stirred yoghurt, Int. J. Food Sci. Technol.34(2) (1999) 137-143.

[9] A.S. Naidu, W.R. Bidlack, R.A. Clemens, Probiotic Spectra of Lactic Acid Bacteria (LAB), Crit. Rev. Food Sci. Nutr. 39(1) (1999) 13-126.

[10] Y. Gharbi, I. Fhoula, P. Ruas-Madiedo, N. Afef, A. Boudabous, M. Gueimonde, H.-I. Ouzari, In-vitro characterization of potentially probiotic Lactobacillus strains isolated from human microbiota: interaction with pathogenic bacteria and the enteric cell line HT29, Ann. Microbiol. 69(1) (2019) 61-72.
[11] H. Jensen, S. Grimmer, K. Naterstad, L. Axelsson, In vitro testing of commercial and potential probiotic lactic acid bacteria, Int. J. Food Microbiol. 153(1) (2012) 216-222.
[12] W.H. Holzapfel, P. Haberer, J. Snel, U. Schillinger, J.H.J. Huis in't Veld, Overview of gut flora and probiotics, International J.Food Microbiol. 41(2) (1998) 85-101.
[13] P. Ruas-Madiedo, J. Hugenholtz, P. Zoon, An overview of the functionality of exopolysaccharides produced by lactic acid bacteria, Int. Dairy J. 12(2) (2002) 163-171.
[14] A. Laws, Y. Gu, V. Marshall, Biosynthesis, characterisation, and design of bacterial exopolysaccharides from lactic acid bacteria, Biotechnology Adv. 19(8) (2001) 597-625.
[15] A.P. Laws, V.M. Marshall, The relevance of exopolysaccharides to the rheological properties in milk fermented with ropy strains of lactic acid bacteria, Int. Dairy J.I 11(9) (2001) 709-721.
[16] G. Caggianiello, M. Kleerebezem, G. Spano, Exopolysaccharides produced by lactic acid bacteria: from health-promoting benefits to stress tolerance mechanisms, Appl. Microbiol. Biotechnol. 100(9) (2016) 3877-3886.
[17] D. Patten, A.P.J.B.M. Laws, Lactobacillus-produced exopolysaccharides and their potential health benefits: a review, Benefic. Microbes6(4) (2015) 457-471.
[18] P. Ruas-Madiedo, C.G. De Los Reyes-Gavilán, Invited review: Methods for the screening, isolation, and characterization of exopolysaccharides produced by lactic acid bacteria, J. Dairy Sci. 88(3) (2005) 843-856.
[19] E.C. Ale, M.J. Perezlindo, Y. Pavón, G.H. Peralta, S. Costa, N. Sabbag, C. Bergamini, J.A. Reinheimer, A.G. Binetti, Technological, rheological and sensory characterizations of a yogurt containing an exopolysaccharide extract from Lactobacillus fermentum Lf2, a new food additive, Food Res. Int. 90 (2016) 259-267.
[20] E.C. Ale, V.A. Batistela, G. Correa Olivar, J.B. Ferrado, S. Sadiq, H.I. Ahmed, J.A. Reinheimer, L. Vera-Candioti, A.P. Laws, A.G. Binetti, Statistical optimisation of the exopolysaccharide production by Lactobacillus fermentum Lf2 and analysis of its chemical composition, Int.J. Dairy Technol. (2019) doi:10.1111/1471-0307.12639.

[21] E.C. Ale, M.J. Perezlindo, P. Burns, E. Tabacman, J.A. Reinheimer, A.G. Binetti, Exopolysaccharide from Lactobacillus fermentum Lf2 and its functional characterization as a yogurt additive, J.Dairy Res. 83(4) (2016) 487-492.
[22] A. Vitlic, S. Sadiq, H.I. Ahmed, E.C. Ale, A.G. Binetti, A. Collett, P.N. Humpreys, A.P. Laws, Isolation and characterization of a high molecular mass β-glucan from Lactobacillus fermentum Lf2 and evaluation of its immunomodulatory activity, Carbohydr. Res. 476 (2019) 44-52.
[23] G.J. Gerwig, J.P. Kamerling, J.F.G. Vliegenthart, Determination of the absolute configuration of monosaccharides in complex carbohydrates by capillary g.l.c, Carbohydr. Res. 77(1) (1979) 1-7.
[24] M. Abdel-Akher, T.K. Hamilton, R. Montgomery, F. Smith, A new procedure for the determination of the fine structure of polysaccharides, J. Am.Chem. Soc. 74(19) (1952) 4970-4971.
[25] J.Ø. Duus, C.H. Gotfredsen, K. Bock, Carbohydrate Structural Determination by NMR Spectroscopy: Modern Methods and Limitations, Chem. Rev. 100(12) (2000) 4589-4614.
[26] D. Wefers, C.E. Tyl, M.J.F.i.c. Bunzel, Novel arabinan and galactan oligosaccharides from dicotyledonous plants, Front. Chem. 2 (2014) 100.
[27] K. Bock, C. Pedersen, Carbon-13 Nuclear Magnetic Resonance Spectroscopy of Monosaccharides, in: R.S. Tipson, D. Horton (Eds.), Adv.Carbohydr. Chem.vBiochem., Academic Press (1983), pp. 27-66.
[28] P.V. Toukach, Bacterial Carbohydrate Structure Database 3: Principles and Realization, J. Chem. Info. Model. 51(1) (2011) 159-170.
[29] M. Pallach, F. Di Lorenzo, F.A. Facchini, D. Gully, E. Giraud, F. Peri, K.A. Duda, A. Molinaro, A. Silipo, Structure and inflammatory activity of the LPS isolated from Acetobacter pasteurianus CIP103108, Int .J.Biol. Macromol. 119 (2018) 1027-1035.
[30] M. Dubois, K. Gilles, J.K. Hamilton, P.A. Rebers, F. Smith, A colorimetric method for the determination of sugars, Nature 168(4265) (1951) 167.
[31] M. Dubois, K.A. Gilles, J.K. Hamilton, P.A. Rebers, F. Smith, Colorimetric Method for Determination of Sugars and Related Substances, Anal. Chem. 28(3) (1956) 350-356.
[32] S. Balzaretti, V. Taverniti, S. Guglielmetti, W. Fiore, M. Minuzzo, H.N. Ngo, J.B. Ngere, S. Sadiq, P.N. Humphreys, A.P. Laws, A novel rhamnose-rich hetero-exopolysaccharide isolated from Lactobacillus paracasei DG activates THP-1 human monocytic cells, Appl.Environ. Microbiol. 83(3) (2017) pii: e02702-16. doi: 10.1128/AEM.02702-16.

[33] K. Stellner, H. Saito, S.I. Hakomori, Determination of aminosugar linkages in glycolipids by methylation. Aminosugar linkages of ceramide pentasaccharides of rabbit erythrocytes and of Forssman antigen, Arch. Biochem. Biophys.155(2) (1973) 464-472.